LANGMUIR

pubs.acs.org/Langmuir Article

Multiphase Coexistences in Rod−Polymer Mixtures

Vincent F. D. Peters, Álvaro González García, Henricus H. Wensink, Mark Vis,* and Remco Tuinier

Cite This: *Langmuir* 2021, 37, 11582−11591

ABSTRACT: Using recently derived analytical equations of state for hard rod dispersions, we predict the phase behavior of athermal rod−polymer mixtures with free volume theory. The rods are modeled as hard spherocylinders, while the nonadsorbing polymer chains are described as penetrable hard spheres. It is demonstrated that all of the different types of phase states that are stable for pure colloidal rod dispersions can coexist with any combination of these phases if polymers are added, depending on the concentrations, rod aspect ratio, and polymer−rod size ratio. This includes novel two-, three-, and four-phase coexistences and isostructural coexistences between dilute and concentrated phases of the same kind, even for the more ordered (liquid) crystal phases. This work provides insight into the conditions at which particular multiphase coexistences are expected for well-defined model colloidal rod−polymer mixtures. We provide a quantitative map detailing the various types of isostructural coexistences, which confirms an early qualitative hypothesis by Bolhuis et al. (*J. Chem. Phys. 107*, **1997** 1551).

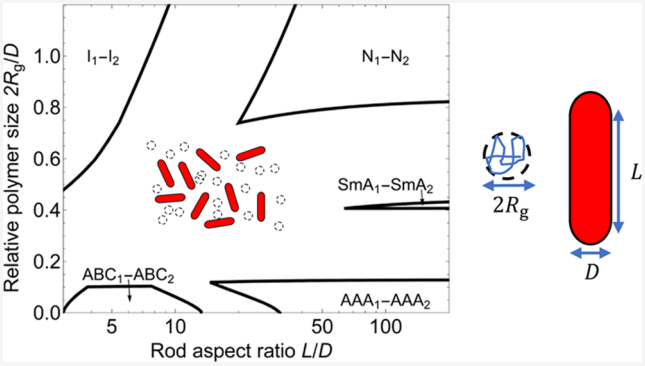

INTRODUCTION

Suspensions of rodlike particles exhibit fascinating phase behavior.[1,2] Addition of nonadsorbing polymers to dispersions of colloidal rodlike particles, like tobacco mosaic[3,4] or filamentous viruses,[5,6] cellulose nanocrystals,[7,8] or boehmite rods,[9] can lead to demixing into two or three coexisting phases in otherwise stable suspensions. Similar to mixtures of spherical colloids and polymers, the phase behavior in rod−polymer mixtures has been explained with the concept of polymer-mediated excluded volume interactions.[10−13] In such mixtures, there is a region around each colloidal particle that is depleted of polymers. When these depletion zones of different colloidal particles overlap, the available volume for the polymers and thus the entropy of the polymer chains increases. As a result, adding nonadsorbing polymers leads to an effective depletion attraction between the colloidal particles. For spherical particles, this depletion effect can lead to phase-separated colloid−polymer mixtures, in which colloidal gas, liquid, and/or crystal phases coexist.[14,15] Similar effects on the phase behavior of rodlike particle dispersions are expected, but because these also exhibit liquid crystalline phases,[16−22] a rich set of possible phase coexistences and system properties is expected as well.

To theoretically quantify the effects of nonadsorbing polymers on the phase behavior of rods, it is useful to model the rodlike particles as hard spherocylinders.[13] In this model, the colloidal rods cannot penetrate each other and do not interact otherwise. Computer simulations[24,25] revealed that dispersions of hard spherocylinders can assume isotropic (I), nematic (N), smectic-A (SmA), AAA, and ABC phase states (see Figure 1 for a sketch of these phase states).[23,25] The thermodynamically preferred phase state depends on the concentration and length−diameter aspect ratio. In both the isotropic and nematic phases, there is no positional order, but in the nematic phase, the rods assume a preferred orientation. Depending on the rod aspect ratio, both I and N phases can be

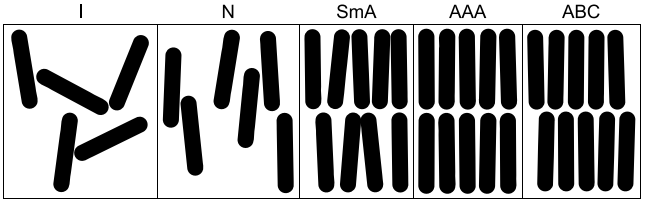

Figure 1. Sketch of the different phase states for hard spherocylinder dispersions from left to right: isotropic (I), nematic (N), smectic-A (SmA), AAA crystal, and ABC crystal. Reprinted figure with permission from Peters et al.[23], *Phys. Rev. E 101*, 062707, **2020**. Copyright 2020 by the American Physical Society.

Received: July 16, 2021
Revised: September 9, 2021
Published: September 23, 2021

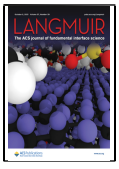

https://doi.org/10.1021/acs.langmuir.1c01896
Langmuir 2021, 37, 11582−11591

observed in dilute dispersions. At somewhat higher colloid concentrations, the rods can assume a smectic-A phase. In this phase state, the particles are confined into layers wherein they move freely while being aligned perpendicular to the layer normal. At even higher concentrations, the rods may form either an AAA or ABC crystal phase with long-range periodic order in all three dimensions. Here, the particles are also confined into layers, but within the layers, there is hexagonal packing. For the AAA phase, rods are packed directly on top of each other. For the ABC phase, the rods are stacked in between the rods of adjacent layers. The resulting ABC packing is equivalent to the FCC crystal phase of spheres. The stability of these particular crystalline phases is related to the spherical geometry of the endcaps. Because the endcaps dictate a small portion of the crystal lattice, there is only a small difference in the free energy of the crystalline phases, especially for longer rods. In experiments, other liquid crystal phases like the smectic-B or columnar phase have also been observed for dispersions of colloidal rods, and this is attributed to polydispersity, semiflexibility, or additional (e.g., electrostatic) interactions.[20,21,26−29]

Most of the experimental and theoretical work on the phase behavior of rod−polymer mixtures focused on the I−N phase coexistence.[6−10,13] These show that the I−N phase coexistence region can broaden upon adding nonadsorbing polymers. For relatively large polymers, the isotropic phase may become unstable at certain compositions, leading to isostructural I_1-I_2 phase equilibria. In an isostructural phase equilibrium, two phases of the same kind but at different concentrations are in equilibrium, similar to a gas−liquid coexistence. In the case of relatively small polymers, earlier theoretical approaches[10,13] also predicted that the nematic phase may become unstable leading to (isostructural) N_1-N_2 equilibria. With regard to the other phase equilibria, the I−SmA coexistence has been reported experimentally as well.[4,5] Additionally, for a limited set of aspect ratios, Monte Carlo simulations were performed on the full phase behavior by Bolhuis et al.[11] and Savenko and Dijkstra.[12] Systematic knowledge about the trends of the phase behavior of rod−polymer mixtures, including the smectic and crystal phases, for a wide range of aspect ratios and polymer sizes, is however still lacking.

Recently, we predicted that for athermal rod−polymer mixtures, four- and five-phase coexistences are obtained that initially seemed in contrast to the Gibbs phase rule, but could be explained using an extended Gibbs phase rule.[30] The work of ref 30, however, only highlights a fraction of the plethora of multiphase coexistences possible for rod−polymer mixtures. Only a limited range of parameters was explored and the isostructural coexistences were out of the scope of that work. Based on the same theoretical methods,[30] here, FVT is combined with recently derived equations of state[23] for the phase states in hard spherocylinder dispersions. For details on this theoretical framework, we refer to the Methods section or ref 30. We aim to systematically map out the trends in the phase behavior for rod−polymer mixtures including isostructural coexistences to indicate which type of (isostructural) phase coexistences can be obtained at certain aspect ratios and polymer sizes. This should aid further experimental or computer simulation work on rod−polymer mixtures to locate a particular coexistence of interest, as it is difficult to scan such a wide range of parameters outside of theoretical methods.

METHODS

Free Volume Theory. We approximate the colloidal rods as hard spherocylinders (HSC) of length L, diameter D (total length $L + D$), and volume $v_c = \pi LD^2/4 + \pi D^3/6$, and the polymers as penetrable hard spheres (PHS) with radius $\delta = R_g$ and volume $v_p = 4\pi\delta^3/3$. The number densities of the colloids and polymers, ρ_c and ρ_p, respectively, are related to the respective volume fractions, $\eta = \rho_c v_c$ and $\phi = \rho_p v_p$. PHS are considered as hard particles regarding interactions with the rods, and thus they cannot penetrate these particles. PHS have no interactions with themselves and can freely overlap with each other, so a dispersion of PHS behaves like an ideal solution.

In FVT, we treat the rod−polymer mixture within a semi-grand canonical ensemble.[10,14] The system of interest of HSC + PHS is in contact with a polymer (PHS) reservoir through a semipermeable membrane that is impermeable to the colloids but fully permeable for the polymers. Solvent is considered as background in both the reservoir and the system. This allows us to derive the following semi-grand canonical potential Ω of the system[14]

$$\omega = \frac{\Omega v_c}{k_B T V} = f^0 - \alpha\tilde{\Pi}^R \tag{1}$$

where ω is the normalized semi-grand canonical potential, k_BT is the thermal energy, V is the total (constant) volume of the system, $f^0 = F^0 v_c/(k_BTV)$ is the normalized Helmholtz free energy of a pure rod dispersion as outlined previously,[23] and $-\alpha\tilde{\Pi}^R$ is the change in ω caused by the presence of polymer in the system. The term Π^R is the osmotic pressure in the polymer reservoir which by approximating the polymers as PHS is given by van't Hoff's law $\Pi^R = \rho_p^R k_B T$ for an ideal solution of polymer particles. The normalized osmotic pressure is therefore given by[13]

$$\tilde{\Pi}^R = \frac{\Pi^R v_c}{k_B T} = \frac{v_c}{v_p}\phi^R = \frac{3\Gamma - 1}{2q^3}\phi^R \tag{2}$$

where $\Gamma = 1 + L/D$ is the relative total rod length (with L/D being the rod aspect ratio) and $q = 2\delta/D$ is the relative polymer size. The quantity $\phi^R = \rho_p^R v_p$ is the relative polymer concentration in the reservoir; $\phi^R = 1$ refers to the polymer coil overlap concentration, related to the relative polymer concentration in the system ϕ by $\phi = \alpha\phi^R$. The term $\alpha = \langle V_{free}\rangle/V$ is the ensemble-averaged free volume available for the polymers normalized to the total system volume. We approximate α by the free volume fraction in the undistorted pure rod dispersion with $\alpha = \langle V_{free}\rangle^0/V$, which is estimated by scaled particle theory as follows[10,13]

$$\alpha = (1 - \eta)\exp(-Q) \tag{3}$$

where η is the rod volume fraction and Q is given by

$$Q = \left(\frac{6q\Gamma}{3\Gamma - 1} + \frac{3q^2(\Gamma + 1)}{3\Gamma - 1}\right)\frac{\eta}{1 - \eta} + \frac{1}{2}\left(\frac{6q\Gamma}{3\Gamma - 1}\frac{\eta}{1 - \eta}\right)^2 + \frac{2q^3\tilde{\Pi}^0}{3\Gamma - 1}$$

Here, $\tilde{\Pi}^0 = \Pi^0 v_c/(k_BT)$, with $\tilde{\Pi}^0$ as the osmotic pressure of a pure rod dispersion, which is estimated from the specific equation of state for the phase of the rods.[23]

Phase Behavior. *Binodals.* From eq 1, it is possible to calculate the concentrations at the binodals from two different phases i and j by solving the coexistence equations

$$\tilde{\mu}_i = \tilde{\mu}_j \tag{4}$$

$$\tilde{\Pi}_i = \tilde{\Pi}_j \tag{5}$$

where $\tilde{\mu} = \mu/(k_BT)$ and $\tilde{\Pi}$ are the normalized colloid chemical potential and normalized osmotic pressure of the colloid−polymer mixture in the system. Chemical equilibrium for the polymers is already implied within the framework of FVT. These thermodynamic

https://doi.org/10.1021/acs.langmuir.1c01896
Langmuir 2021, 37, 11582−11591

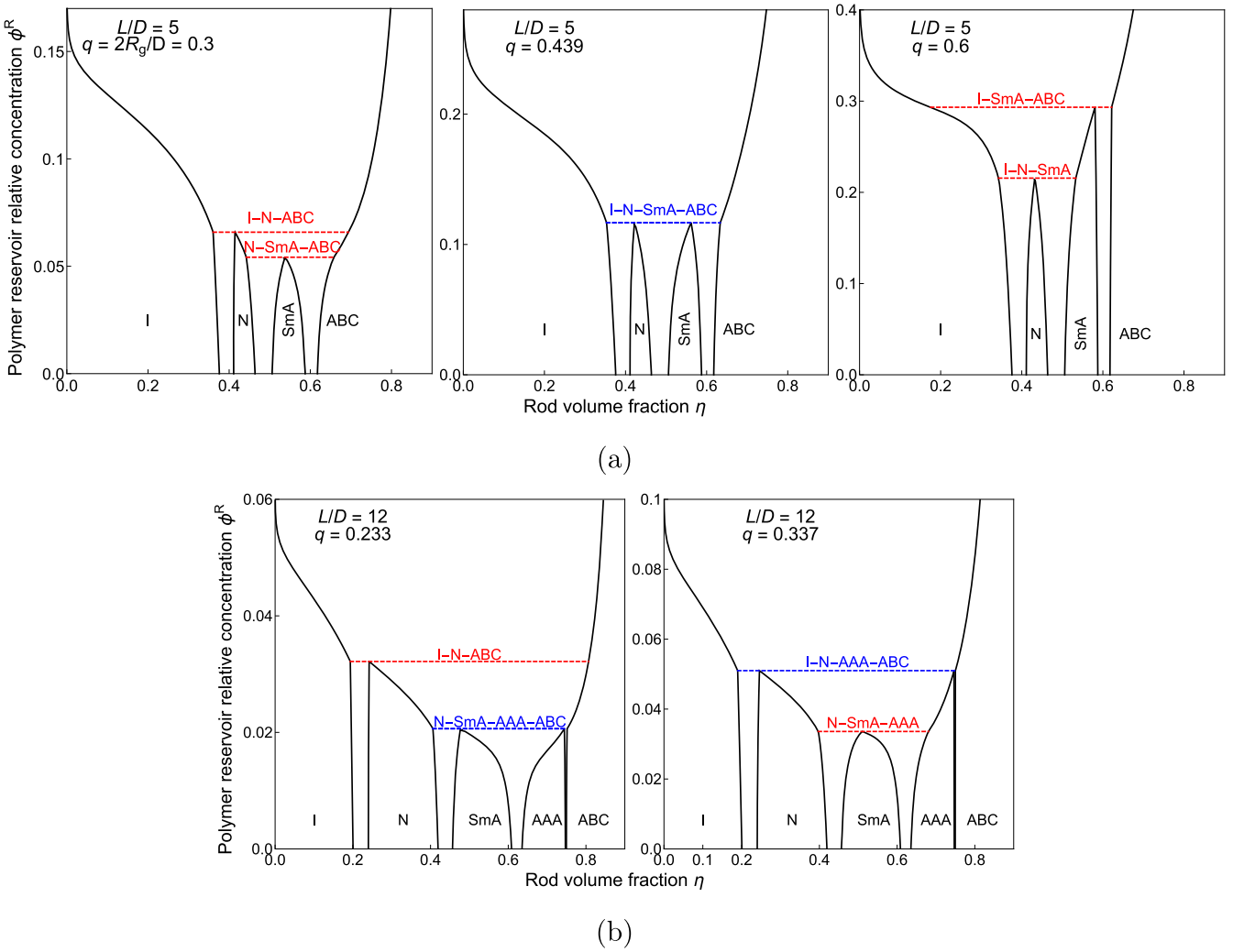

Figure 2. Phase diagrams of dispersions of rods modeled as hard spherocylinders with rod length-to-diameter ratio (a) $L/D = 5$ or (b) $L/D = 12$ plus nonadsorbing polymers described as penetrable hard spheres. The binodals (solid curves) are plotted in terms of the polymer reservoir relative concentration ϕ^R versus rod volume fraction η for various relative polymer sizes $q = 2R_g/D$. Three- and four-phase coexistences are indicated with, respectively, red or blue dashed horizontal lines. The isotropic (I), nematic (N), smectic-A (SmA), AAA crystal, and ABC crystal phase states of the rods are considered.

quantities can be obtained from ω in eq 1 using $\tilde{\mu} = \partial\omega/\partial\eta$, $\tilde{\Pi} = -\partial(\omega/\eta)/\partial(1/\eta)$[14]

$$\tilde{\mu} = \tilde{\mu}^0 - \tilde{\Pi}^R \frac{\partial\alpha}{\partial\eta} \tag{6}$$

$$\tilde{\Pi} = \tilde{\Pi}^0 + \tilde{\Pi}^R\left(\alpha - \eta\frac{\partial\alpha}{\partial\eta}\right) \tag{7}$$

With eqs 4 and 5, the concentrations η_i and η_j can then be predicted for all two-phase coexistences as a function of ϕ^R, q, and Γ. At certain values of these parameters, coexistence between more than two phases is possible. In such cases, the additional coexisting phases should also have the same $\tilde{\mu}$ and $\tilde{\Pi}$. The equations $\tilde{\mu}_i = \tilde{\mu}_k$ and $\tilde{\Pi}_i = \tilde{\Pi}_k$ should be solved for all involved phases k, so the preferred phase state or phase coexistence at specific system parameters is the one with the lowest ω, while the others are metastable.

Isostructural Coexistence. Under certain conditions, a single phase may demix into a dilute and concentrated version of the same phase state, e.g., I_1–I_2 coexistence, like how a fluid demixes into gas and liquid phases. These binodals can also be calculated using eqs 4 and 5. The conditions for which the composition of the two coexisting isostructural phases becomes identical is known as the critical point, which is obtained by

$$\frac{\partial^2\omega}{\partial\eta^2} = \frac{\partial^3\omega}{\partial\eta^3} = 0 \tag{8}$$

For certain values of q and Γ, it is however possible that other phase coexistences are more stable than the isostructural phase coexistence at the critical point. In such a case, the isostructural phase coexistence is metastable at all concentrations. For example, under certain conditions, the I–N coexistence is preferred over the I_1–I_2 coexistence. To identify the conditions at which the critical point is at the verge of becoming more favorable than another phase coexistence, it is useful to calculate the critical endpoint (CEP). At the CEP, the critical point coexists with another phase state, so eqs 4, 5, and 8 apply simultaneously. For instance, the CEP of I–N coexistence at the I_1–I_2 critical point is given by solving $\partial^2\omega_I/\partial\eta^2 = \partial^3\omega_I/\partial\eta^3 = 0$, $\tilde{\mu}_I = \tilde{\mu}_N$, and $\tilde{\Pi}_I = \tilde{\Pi}_N$. When q is increased above q_{CEP}, I_1–I_2 coexistence will, at least at certain compositions, be preferred over I–N coexistence.

RESULTS

Phase coexistences have been predicted for hard spherocylinders mixed with polymers for a wide variety of rod aspect ratios L/D and polymer-to-rod size ratio $q = 2R_g/D$. Here, D is the rod diameter, L is the rod length (excluding hemispherical

https://doi.org/10.1021/acs.langmuir.1c01896
Langmuir 2021, 37, 11582–11591

endcaps), and R_g is the polymer radius of gyration. In the following, we provide illustrative phase diagrams for the different stable phase coexistences and elaborate on the trends in phase behavior upon changing the system parameters. First, we focus on the phase behavior at the specific range of parameters where isostructural coexistence is not predicted.

Nonisostructural Phase Coexistence. In Figure 2a, we have plotted three representative phase diagrams of rods with $L/D = 5$ mixed with polymers of various (relative) polymer sizes q. They indicate the variety of phase coexistences that can occur upon changing q and also indicate a four-phase coexistence. The different phase states and phase coexistences are marked in the plots, where the solid curves represent binodals and the dashed lines indicate where the binodals coincide to give three- or four-phase coexistences.

At low polymer concentrations, the same coexistences are found as in pure rod dispersions. Here, it follows that the isotropic (I), nematic (N), smectic-A (SmA), and ABC crystal phases are the preferred phase states found upon increasing the rod concentration.[23−25] In between these single-phase states are regions of two-phase coexistence. For example, we predict an I−N coexistence between $\eta \approx 0.37-0.41$ for pure rod dispersions. As the polymer concentration is increased, the region of I−N phase coexistence widens. For $q = 0.3$ (Figure 2a, left), an I−N−ABC triple line is predicted near $\phi^R \approx 0.07$. At higher polymer concentrations, the N phase is metastable and I−ABC phase coexistence is found instead. For the N−SmA and SmA−ABC phase coexistence, similar trends can be observed: both regions of two-phase coexistences widen as the polymer concentration is increased. At $q = 0.3$, an N−SmA−ABC triple line is obtained when the N−SmA and SmA−ABC coexistences coincide at $\phi^R \approx 0.05$. Upon further increase of the polymer concentration, the SmA phase becomes metastable and instead an N−ABC coexistence appears. The N−ABC phase coexistence is only found for ϕ^R values below the I−N−ABC triple line, as at higher ϕ^R, only I−ABC coexistence remains.

At $q = 0.6$ (Figure 2a, right), different triple lines are predicted instead with the I−SmA−ABC and I−N−SmA coexistence. At polymer concentrations between these triple lines, the I−SmA phase coexistence is predicted. In comparing these graphs, it is useful to define the relative stability. At $q = 0.3$, the single-phase N region is stable at higher values of ϕ^R than the single-phase SmA region, while at $q = 0.6$, it is the other way around. The relative height of the peaks of these regions dictates what kind of coexistences are found. We indicate this by saying that at $q = 0.3$, the N phase is relatively more stable upon increasing ϕ^R than the SmA phase, and vice versa at $q = 0.6$. Furthermore, we can conclude that the relative stability of the SmA phase compared to the N phase has increased upon increasing q.

Exactly at $q = 0.439$ (Figure 2a, middle), the relative stability of the N and SmA phase is the same. Hence, a quadruple line is found since the I−N−ABC, N−SmA−ABC, I−N−SmA, and I−SmA−ABC triple lines have merged. For this reason, the two-phase N−ABC or I−SmA coexistences do not appear in this case. The principle behind the four-phase I−N−SmA−ABC coexistence is similar to that reported for plate−polymer mixtures[31] and the I−N−SmA−AAA coexistence reported for rod−polymer mixtures.[30] However, for the plate−polymer mixtures of ref 31, only three structurally different phases were considered, so four-phase coexistence was solely observed in combination with an isostructural coexistence.

These multiphase coexistences occur only at a particular colloid and polymer chemical potential and osmotic pressure and therefore at a particular value of the polymer reservoir concentration ϕ^R. Hence, the multiphase coexistences are found only along the dashed lines in this representation. The polymer concentration in the system, given by $\phi = \alpha\phi^R$, is different for different values of colloid volume fractions η, since the free volume fraction α is a function of η. Therefore, the triple or quadruple points become a region in the system representation with a range of η and ϕ. Within this region, the system can demix into these particular phases of fixed composition but with varying volumes.

Even more different coexistences that have not been reported before emerge at $L/D = 12$ (see Figure 2b) and relatively small q values. Here, at low polymer concentrations and in pure rod dispersions[23] the N and SmA phases are stable over a wider range of η in comparison to $L/D = 5$. Additionally, the AAA crystal phase now precedes the ABC crystal phase for $\eta \approx 0.63-0.75$. We observe similar trends in coexistences as for $L/D = 5$ (see Figure 2a). The two-phase coexistence regions, N−SmA and SmA−AAA in particular, widen as the polymer concentration is increased and depending on the relative stability of the N, SmA, and AAA phases upon increasing ϕ^R, different phase coexistences than before are stable. At $q = 0.233$, there is now an N−SmA−AAA−ABC quadruple line, and at $q = 0.337$, there is an I−N−AAA−ABC quadruple line. Additionally, we find I−N−ABC or N−SmA−AAA triple lines, and at intermediate ϕ^R values, there is N−ABC or N−AAA two-phase coexistence.

These coexistences are all dictated by the relative stability of the N, SmA, and AAA phase upon increasing ϕ^R. For example, at exactly $q = 0.233$, the relative stability of the AAA phase upon increasing ϕ^R is equal to that of the SmA phase and lower than that of the N phase. Exactly at $q = 0.337$, the relative stability of the AAA phase is the same as that of the N phase and higher than that of the SmA phase. Here, it is observed that the relative stability of the AAA phase compared to the N and SmA phase is significantly higher for larger q. For even higher q than shown here, the relative stability of the AAA phase only increases further compared to the N and SmA phases, and as for $L/D = 5$, the relative stability of the SmA phase will become higher than for the N phase as well. Therefore, it seems that at larger q, the stability of the more ordered phases increases relative to that of the more disordered phases.

At only these two L/D values and by varying q, we found that all 10 possible combinations of two- and three-phase coexistences can appear (not all are shown in Figure 2). All five possible quadruple lines were also found to appear, although the I−SmA−AAA−ABC coexistence only appears for a narrow range of intermediate L/D values. To indicate when the possible nonisostructural multiphase coexistences appear over a wide range of system parameters, we have calculated the four-phase coexistence points as a function of q and D/L as shown in Figure 3. The different regions in this plot indicate the relative stability of the N, SmA, and AAA phases upon increasing ϕ^R and the different sets of two- and three-phase coexistences, which are described in Table 1. Note that the coexistences found in pure rod dispersions and the I−ABC coexistence are not included as these are not unique to specific regions.

The results in Figure 2a at $L/D = 5$ and $q = 0.3$ or $q = 0.6$ are illustrative to those found in region II or region I,

https://doi.org/10.1021/acs.langmuir.1c01896
Langmuir 2021, 37, 11582−11591

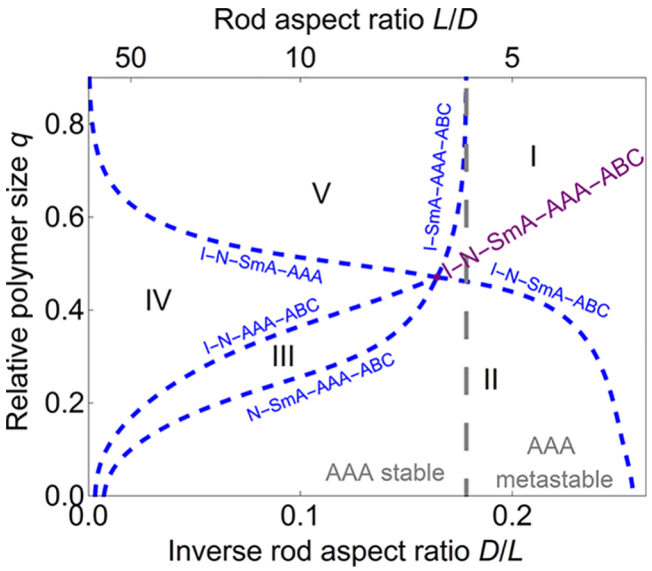

Figure 3. Phase coexistence overview, which, together with Table 1, indicates the possible multiphase coexistences and the relative stability of the N, SmA, and AAA phases upon increasing ϕ^R. The short dashed curves correspond to the four-phase coexistence points, and their intersection (purple) indicates the five-phase coexistence. The vertical long dashed line at $D/L \approx 0.18$ is the SmA−AAA−ABC triple line for pure rod dispersions that shows whether the AAA phase is stable (left) or metastable (right).

respectively, while $q = 0.439$ corresponds to the transition between these regions where a four-phase coexistence is found. Similarly, in Figure 2b, at $L/D = 12$, we have shown the transition between regions II and III at $q = 0.233$ and between regions III and IV at $q = 0.337$. At $L/D = 6.086$ and $q = 0.470$, all quadruple curves converge to form the five-phase coexistence reported earlier.[30]

In the region of short rods at $D/L \gtrsim 0.18$, there is only the I−N−SmA−ABC four-phase coexistence as the AAA phase is metastable. This curve indicates the parameters where either the N or SmA phase is more stable upon increasing ϕ^R. At $D/L \approx 0.26$, the q value of the I−N−SmA−ABC coexistence vanishes because D/L then approaches the I−N−SmA triple line for pure rod dispersions.[23] At higher D/L, the N phase becomes metastable. For longer rods at lower D/L, the I−N−SmA−ABC four-phase coexistence becomes metastable as the relative stability of the AAA phase becomes larger. Here, the I−N−SmA−AAA curve instead indicates whether the N or SmA phase is more stable with respect to ϕ^R. For long rods, the value of q increases rapidly and the SmA phase will only be more stable than the N phase for relatively large polymers.

The I−SmA−AAA−ABC and N−SmA−AAA−ABC curves designate whether the SmA or AAA phase is the preferred phase state. Similar to I−N−SmA−ABC coexistence, the I−SmA−AAA−ABC curve increases asymptotically when approaching the SmA−AAA−ABC triple line for pure rod dispersions at $D/L \approx 0.18$. The N−SmA−AAA−ABC curve goes to $q = 0$ at $L/D \approx 138$. Finally, only the I−N−AAA−ABC curve designates whether the N or AAA phase is more stable. Note that the relative stability between these two phases is not relevant within region I with regard to different phase coexistences, and it is therefore not indicated. The I−N−AAA−ABC curve attains $q = 0$ at $L/D \approx 325$. At $L/D \gtrsim 325$ or $D/L \lesssim 0.003$, the AAA phase is thus always the preferred phase state compared to the N and SmA phase with respect to ϕ^R.

The relative stability of the N, SmA, and AAA phases in rod−polymer mixtures can be summarized as follows: for short rods and large polymers, the SmA phase is the most stable; for short or long rods and small polymers, the N phase is the thermodynamically preferred state; and for long rods and large polymers or very long rods and all polymer sizes, the AAA phase is the most stable. In general, increasing the polymer size tends to promote the stability of ordered phases over disordered ones.

Phase Behavior Including Isostructural Phases. The size ratios used to calculate the illustrative phase diagrams in Figure 2 have been chosen intentionally such that isostructural phase coexistences are metastable. These isostructural coexistences also do not interfere with any of the quadruple lines shown in Figure 3. In general, it is not obvious whether isostructural phase equilibria are metastable or not. For quite some time, the fluid−fluid phase coexistence in binary hard sphere mixtures was a matter of debate until computer simulations of Dijkstra, van Roij, and Evans[32] revealed they are metastable. Here, we show that isostructural phase equilibria can appear (are not metastable) for all five phase states of the rods. In the following, we show illustrative phase diagrams for all of these possible isostructural phase coexistences and indicate at which size parameters these are preferred.

For $L/D = 4.5$, the I_1−I_2 coexistence only appears in phase diagrams for $q > 0.636$ (critical endpoint). In Figure 4a, we show an example of a phase diagram that reveals an isostructural phase coexistence at $L/D = 4.5$ at a q value of 0.728 (so relatively long-range attraction). Near $\phi^R \approx 0.36$ and $\eta \approx 0.2$, there is a critical point above which it becomes favorable that the isotropic phase demixes into a dilute (I_1) and concentrated (I_2) isotropic phase. As the polymer concentration increases, the I_1−I_2 coexistence region widens. At $\phi^R \approx 0.43$, the I_1−I_2−N−SmA quadruple line is reached and the I_2 phase becomes metastable with increasing polymer concentrations. Additionally, there is an I_1−SmA−ABC triple line and I_1−SmA at intermediate polymer concentrations.

Again it is the relative stability upon increasing ϕ^R of the different phases that determines which kind of coexistences are

Table 1. Relative Stabilities of the N, SmA, and AAA Phases upon Increasing ϕ^R and the Unique Stable Phase Coexistences Are Given for the Specified Regions in Figure 3

		type of phase coexistence				
region	relative stability	two phases		three phases		
I	SmA > N and SmA > AAA	I−SmA	SmA−ABC	I−N−SmA	I−SmA−ABC	SmA−AAA−ABC
II	N > SmA > AAA	N−ABC	SmA−ABC	I−N−ABC	N−SmA−ABC	SmA−AAA−ABC
III	N > AAA > SmA	N−AAA	N−ABC	I−N−ABC	N−SmA−AAA	N−AAA−ABC
IV	AAA > N > SmA	I−AAA	N−AAA	I−N−AAA	N−SmA−AAA	I−AAA−ABC
V	AAA > SmA > N	I−SmA	I−AAA	I−N−SmA	I−SmA−AAA	I−AAA−ABC

https://doi.org/10.1021/acs.langmuir.1c01896
Langmuir 2021, 37, 11582−11591

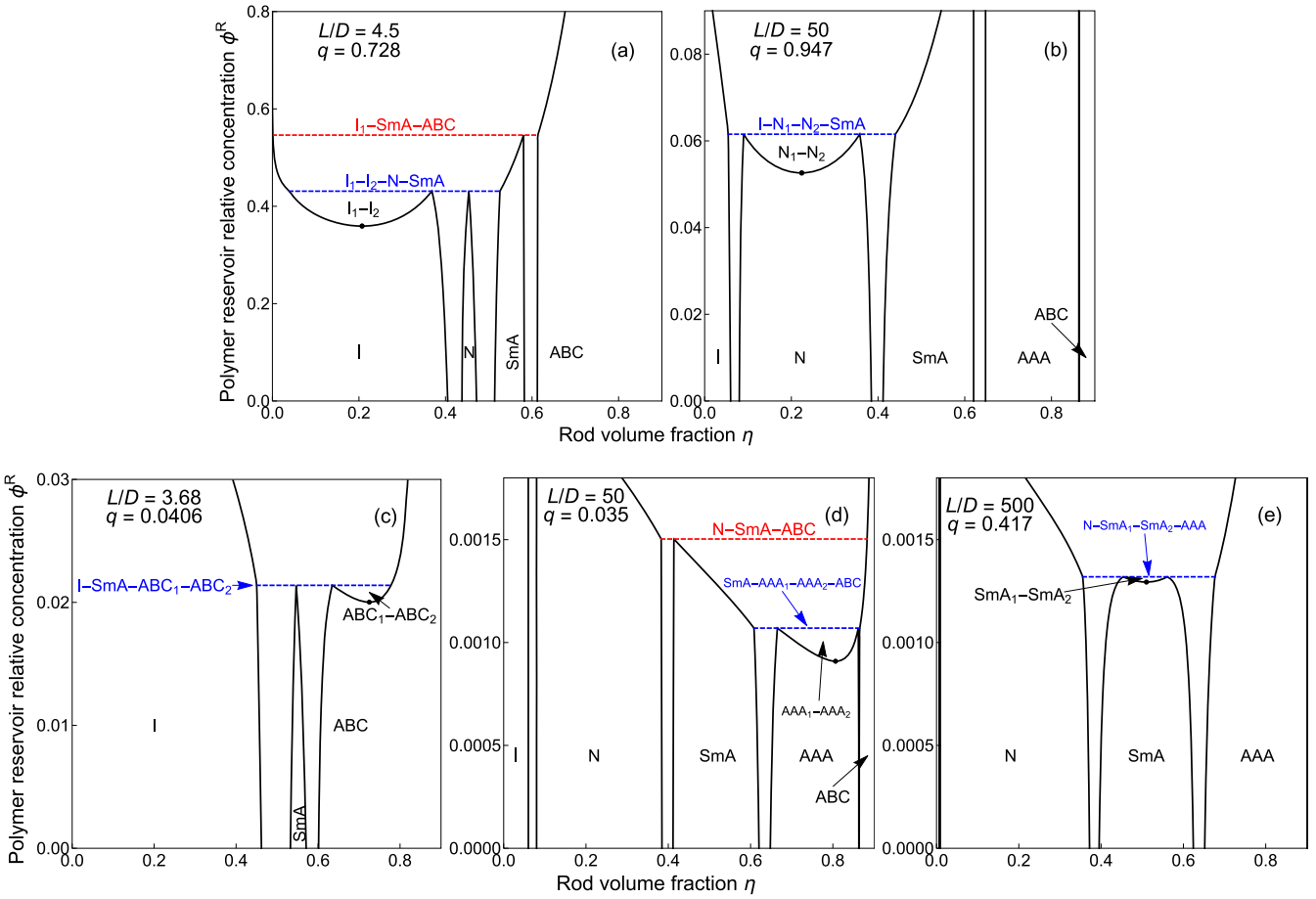

Figure 4. Phase diagrams as in Figure 2, but for different q and L/D values indicated in the plots, focusing on conditions with isostructural phase coexistence. A distinction is made between a dilute (I_1, N_1,SmA_1, AAA_1, ABC_1) and concentrated (I_2, N_2, SmA_2, AAA_2, ABC_2) phase state. The critical points of isostructural phase coexistences are indicated by filled circles.

found. Now, however, the relative stability that is related to the peak of the I_2 phase is also relevant. At $q = 0.728$, the relative stability of the I_2 and N phases is the same to form the I_1−I_2−N−SmA quadruple line. For other q values, the relative stabilities shift and several other two- and three-phase coexistences can be observed. For increasing q values, two observations were made. First, the I_1−I_2 coexistence region increases as q increases. Second, as q increases, the more highly ordered phases will become more stable with respect to the disordered I_2 phase, which is in agreement with our conclusion in the previous section.

For longer rods and similar q values, a low concentration (N_1) nematic phase coexists with a high concentration nematic (N_2). At $L/D = 50$, the N_1−N_2 coexistence is stable for $0.792 < q < 1.483$. In Figure 4b, an illustrative phase diagram is shown for $q = 0.947$, where an I−N_1−N_2−SmA quadruple line appears. At different q values, novel two- and three-phase coexistences related with the N_1 and N_2 phase can also be found. For both lower and higher q values, the N_1−N_2 coexistence region will become smaller. This time the appearance of certain coexistences is dictated by the relative stability upon increasing ϕ^R of the different peaks for the N_1 and N_2 phase states and the four-phase coexistence in the top right panel is formed when the relative stability is the same. It was observed that as q increases, the relative stability of the N_2 phase increases with respect to the N_1 phase, while both have a lower relative stability compared to the SmA and AAA phase for the entire q stability range ($0.792 < q < 1.483$).

While isostructural coexistences for the I and N phase were reported before,[9−13] we have also found regions for stable isostructural coexistences with the other phase states. In Figure 4, examples of phase diagrams with ABC_1−ABC_2, AAA_1−AAA_2, and SmA_1−SmA_2 isostructural coexistences are presented at a q value where there is four-phase coexistence. For short rods, at $L/D = 3.68$, an ABC_1−ABC_2 coexistence region is observed for small polymers at $q < 0.0906$ (see Figure 4c). At exactly $q = 0.0406$, the stability with respect to ϕ^R of the ABC_1 phase is equal to that of the SmA phase and an I−SmA−ABC_1−ABC_2 coexistence is predicted.

For longer rods, at $L/D = 50$, an AAA_1−AAA_2 coexistence is found instead for small polymers at $q < 0.126$. At exactly $q = 0.035$ (Figure 4d), the stability with respect to ϕ^R of the AAA_1 and AAA_2 phase is equal to find a SmA−AAA_1−AAA_2−ABC quadruple line. In general, ABC_1−ABC_2 coexistence is found for short rods in the opposite limit of both q and η as the I_1−I_2 coexistence. While for longer rods, the AAA_1−AAA_2 coexistence is similarly related to the N_1−N_2 coexistence. For even longer rods, at $L/D = 500$ (Figure 4e), isostructural coexistence for the SmA phase was found for intermediate polymer sized at $0.439776 < q < 0.406952$. At exactly $q = 0.417$, an N−SmA_1−SmA_2−AAA quadruple line is found, where the stability with respect to ϕ^R of the SmA_1 and SmA_2 phases is the same. Note that the coexistence region is tiny.

https://doi.org/10.1021/acs.langmuir.1c01896
Langmuir 2021, 37, 11582−11591

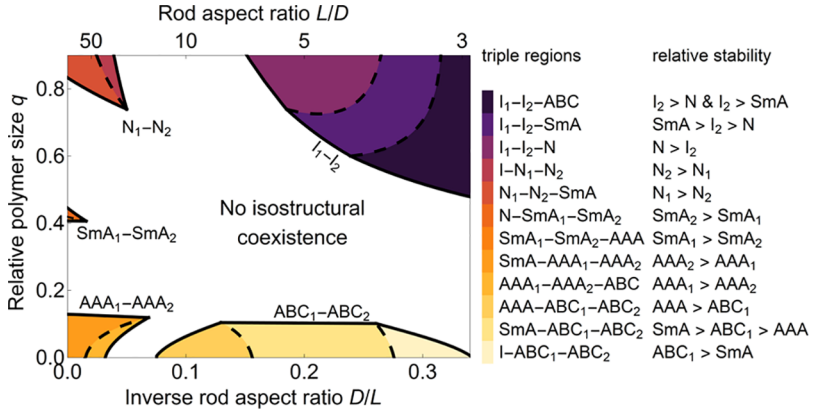

Figure 5. Phase behavior topology overview indicating the stable isostructural coexistences and the relative stability of the relevant dilute and concentrated phases upon increasing ϕ^R. The critical endpoints (solid curves) and four-phase coexistence points (dashed curves) enclose the colored regions where the indicated isostructural phase coexistences are stable.

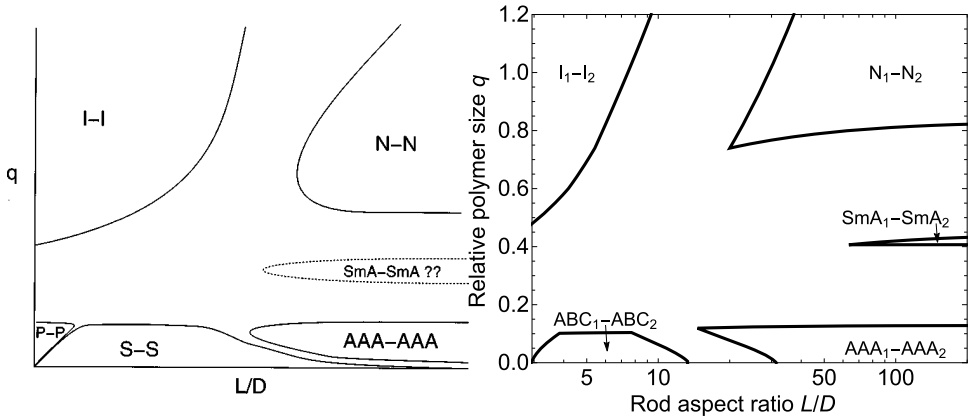

Figure 6. Phase behavior topology overview indicating the stable isostructural two-phase coexistences as speculated by Bolhuis et al. (left)[11] compared to our results (right). Note that the horizontal axis is inverted with respect to the graph in Figure 5. The S−S coexistence denotes the ABC_1−ABC_2 coexistence, while the P−P coexistence refers to a plastic crystal phase only observed for shorter rods than those examined here. The figure on the left reproduced from Bolhuis et al.,[11] with the permission of AIP Publishing.

Even if an experimental, nearly monodisperse, rod−polymer mixture could be realized at the appropriate dimensions, it would still be a challenge to detect this four-phase coexistence region. At this L/D, the I and ABC phase are also only stable at respectively extremely dilute or highly concentrated colloid volume fractions.

To indicate when the different isostructural coexistences and related two-, three-, and four-phase coexistences are found over a wide parameter range, the critical endpoints and quadruple points were predicted as a function of q and L/D as presented in Figure 5. Only at the L/D and q within the colored regions a specific isostructural coexistence is predicted to be stable for certain concentrations. Four-phase coexistence curves involving isostructural coexistence (dashed curves), divide these regions to indicate which specific three-phase coexistence is predicted. Related unique two- and four-phase coexistences can be derived from the triple lines but have been left out for clarity. For instance, in the region where the I_1−I_2−N triple coexistence is found, both an I_1−N and I_2−N coexistence are predicted. On the dashed curve that divides this region with that for the I_1−I_2−SmA triple line, we find I_1−I_2−N−SmA coexistence. The results from Figure 4 can all be linked to one of these region boundaries as in Figure 3. With both phase coexistence overviews (Figures 3 and 5), the complete topology of a phase diagram for a particular L/D and q combination is predicted.

Looking into preferred phase behavior trends, we find that long rods favor N, SmA, and AAA isostructural coexistences and short rods favor I and ABC isostructural coexistences. We also find that some of the trends about relative stability for increasing q, as mentioned before, are found over the entire L/D range. For N, SmA, and AAA isostructural coexistences, it is the case that as q increases, the more concentrated phase becomes more stable with respect to ϕ^R than the more dilute phase. For I and ABC isostructural coexistences, we find that as q increases, the more ordered phase becomes more stable upon increasing ϕ^R than the more disordered phase. As the ordered phases are also more concentrated than the disordered phases in these cases, this is in agreement with the results in Figure 3. In this regard, it is interesting that the isostructural coexistences of the ordered AAA and ABC phases are observed at a small q, for which the stability of strongly ordered phases is relatively low. Similarly, when the more disordered phases have relatively low stability at a high q, isostructural coexistence of the disordered I and N phases is predicted. Further, for long rods at intermediate $q \approx 0.4$, the SmA phase stability is relatively low and SmA_1−SmA_2 coexistence is observed. Thus, for q values at which the stability of a certain phase upon

https://doi.org/10.1021/acs.langmuir.1c01896
Langmuir 2021, 37, 11582−11591

increasing ϕ^R is low compared to other phases, isostructural coexistence becomes more preferred.

DISCUSSION

Figure 6 (right) replots the results from Figure 5 with a different abscissa and without the quadruple lines and the indications of the different additional coexistences. This allows for a clear comparison to a speculative qualitative sketch (left) that was presented in the work of Bolhuis et al.,[11] based upon their computer simulation results for a limited set of conditions. Only for the I_1-I_2 and N_1-N_2 were they able to predict phase diagrams in their paper. It is remarkable how good the agreement is with the graph we are now able to calculate. The trends seem to follow a generic rule of thumb. Isostructural demixing of a certain phase is caused if the size of the added polymer is comparable to the typical distance between the particles in that phase. Then, large polymers will destabilize the more fluid-like phases (I and N) while short polymers generate demixing of the dense AAA/ABC crystals, with demixing of the partially crystalline SmA phase occurring at intermediate polymer sizes. Additionally, our results are also in good agreement with predictions of the phase diagrams themselves computed by the combination of indirect Monte Carlo computer simulations and FVT,[11,12] but these were only reported for a limited number of system parameters. The theoretical framework presented here is also consistent with previous predictions by free volume theory (FVT) for the I−N coexistence.[6,9,13]

The agreement with the sketch in Figure 6 leads us to speculate further over why certain trends in the phase behavior are found using the concepts of excluded volume interactions and FVT. The depletion attraction occurs when the depletion zones around the rods overlap and thus the free volume and entropy for the polymers is increased. The range of the depletion attraction is determined by the size of the depletant, while the strength of this attraction is also related to the osmotic pressure (hence concentration) of the dispersion of depletants, which for our system in turn is related to ϕ^R. We can consider the phase stability upon increasing ϕ^R for a dilute and a concentrated colloidal phase. For small polymers (low q), there is relatively little overlap of depletion zones in both phases and thus there is a significant gain in free volume and polymer entropy when bringing the rods closer together. Due to the proximity of the rods and lower colloidal entropy in the concentrated phase, it is possible that this would require a smaller colloidal entropy loss than for the dilute phase. Therefore, the attraction strength and ϕ^R needed to destabilize the concentrated phase would be lower than for the dilute phase. For large polymers (high q), the concentrated phase has a significant amount of overlap between the depletion zones, while this is not the case for the dilute phase. Therefore, there is only a relatively small gain in free volume and polymer entropy when bringing the rods in the concentrated phase closer together, as the free volume fraction is small in all cases. The attraction strength needed to destabilize the concentrated phase would be higher than that for the dilute phase. Thus, as q increases, dilute and disordered phases become less stable compared to concentrated and ordered phases.

The exact stability of a certain phase is also strongly influenced by the η and L/D values, where this phase is stable in pure rod dispersions. As an example, we consider a phase that is only stable for a small η range, when the L/D is near the triple lines in pure rod dispersions. As this phase is almost metastable already, it requires a small amount of attraction strength for another phase equilibrium to appear. This explains the asymptotic increase in q of the I−SmA−AAA−ABC curve in Figure 3, and the $I_1-I_2-N-SmA$ and $I_1-I_2-SmA-ABC$ curves in Figure 5 near the D/L of, respectively, the SmA−AAA−ABC, I−N−SmA, and I−SmA−ABC triple line for pure rod dispersions. Since here the N, SmA, or AAA phase is only stable at a short range of η, it requires a relatively low ϕ^R to become completely metastable. Thus, even at a higher q, the more ordered N, SmA, or AAA phase is less stable than the more disordered phases. A similar argument can be made for the I−N−SmA−ABC curve going to $q = 0$ near the I−N−SmA triple line for pure rod dispersions.

The range of η also has influence on the appearance of isostructural coexistence. At a lower D/L, the I and ABC phases become stable over a smaller region of η, while the N, SmA, and AAA phases become stable over a larger region of η. Hence, an isostructural coexistence can occur with a larger concentration difference for the N, SmA, and AAA phases than for the I and ABC phases. This makes the I and ABC isostructural coexistences the most stable for short rods, while N, SmA, and AAA isostructural coexistences are the preferred stable phase states for long rods.

While our approach has expanded the range of system parameters for predictions about rod−polymer phase behavior, it should be stressed that due to the theoretical approximations made, only semiquantitative and qualitative agreement with experimental systems is expected. Including effects of polydispersity, polymer−polymer interactions, rod semiflexibility, double-layer interactions in case of charged rods, van der Waals attractions between rods, and the presence of short repulsive anchored brushes is nontrivial within FVT. These could suppress certain phases in favor of other phase symmetries (such as columnar or smectic-B) not considered in our model. It is possible that trends would be shifted and four- or five-phase coexistence can occur for a broader range of q and L/D values. Some of these effects have however been examined within FVT.

For sufficiently large polymer sizes, it is known that the interactions between polymers themselves affect the overall phase behavior from previous calculations on spherical colloid−polymer mixtures. Then, the approximation of polymers as penetrable hard spheres (PHS) is less adequate.[33,34] This leads to an offset of the critical endpoint for the colloidal gas−liquid coexistence. The effect of the polymer interactions could be implemented for rod−polymer mixtures similarly and would likely shift the critical endpoints of the disordered I and N phases to higher q values as was shown in preliminary calculations for I_1-I_2 coexistence.[15] There is however no indication in the reported results on interacting polymers[15,33,34] that it would negate the appearance of the multiphase coexistences altogether; it is expected only to be a quantitative effect.

Also for small polymers, some deviations are expected due to our definition of the free volume fraction α for the more highly ordered phases. This comes from the fact that the expression assumes a fluid-like colloidal phase and does not take into account the correct partitioning of the polymers. A geometrical calculation of α in mixtures of PHS with colloidal spheres[35] or plates[36] was shown to be more accurate for more highly ordered phases. Therefore, we expect a geometrically based α to lead to a shift of the critical endpoints from SmA, AAA, and ABC isostructural coexistence. We wish to underline that these

https://doi.org/10.1021/acs.langmuir.1c01896
Langmuir 2021, 37, 11582−11591

technical modifications will severely complicate the analysis without affecting the qualitative phase behavior trends.

With regard to experimental systems, we should also address the topic of polydispersity as the four- and five-phase coexistences appear at very specific values of L/D and q. While sufficiently monodisperse colloidal particles may be difficult to realize, polydispersity is known to promote multiphase coexistence even further,[37] so it is hypothesized that realistic hard rod−polymer mixtures may indeed reveal the multiphase coexistences for the right parameters under the appropriate conditions. However, the presence of rod length dispersity will likely suppress the formation of the AAA/ABC crystals (and possibly also SmA) in favor of columnar order.[38] Polymer polydispersity often only leads to a quantitative shift in colloid−polymer mixture phase behavior.[39,40]

CONCLUDING REMARKS

Using free volume theory, we have presented a complete map of possible phase coexistences in mixtures of colloidal rods and nonadsorbing polymers with arbitrary rod aspect ratio and rod−polymer size ratio. Due to the inclusion of more strongly ordered (liquid) crystal phases, a plethora of novel two-, three-, and four-phase coexistences are found. We can indicate the conditions where any of the five-phase symmetries for hard spherocylindrical rods (isotropic, nematic, smectic-A, and two crystal states) can be made to coexist with one another. We further show that the addition of polymers is capable of generating isostructural demixing even for the more strongly ordered (liquid) crystal phases, and we can indicate at which conditions they could be found. In further computer simulation studies, the phase coexistences found for short rods are probably most accessible. From an experimental point of view, phase coexistences involving AAA and ABC crystals could be relevant for colloidal rods with a highly monodisperse rod shape mixed with nonadsorbing polymers, while isostructural demixing of the I and N fluids as well as the lamellar SmA structures should be more broadly observable in experimental rod−polymer mixtures with low to moderate size dispersity. Overall, our results highlight the wide range of possibilities in colloidal phase behavior for rod−polymer mixtures and indicate the approximate conditions for obtaining these in realistic systems.

AUTHOR INFORMATION

Corresponding Author

Mark Vis − *Laboratory of Physical Chemistry, Department of Chemical Engineering and Chemistry & Institute for Complex Molecular Systems, Eindhoven University of Technology, 5600 MB Eindhoven, The Netherlands;* orcid.org/0000-0002-2992-1175; Email: m.vis@tue.nl

Authors

Vincent F. D. Peters − *Laboratory of Physical Chemistry, Department of Chemical Engineering and Chemistry & Institute for Complex Molecular Systems, Eindhoven University of Technology, 5600 MB Eindhoven, The Netherlands;* orcid.org/0000-0002-9722-1461

Álvaro González García − *Sustainable Polymer Chemistry Group, Department of Molecules & Materials, MESA + Institute for Nanotechnology, University of Twente, 7500 AE Enschede, The Netherlands*

Henricus H. Wensink − *Laboratoire de Physique des Solides − UMR 8502, CNRS & Université Paris-Saclay, 91400 Orsay, France;* orcid.org/0000-0001-6284-7168

Remco Tuinier − *Laboratory of Physical Chemistry, Department of Chemical Engineering and Chemistry & Institute for Complex Molecular Systems, Eindhoven University of Technology, 5600 MB Eindhoven, The Netherlands;* orcid.org/0000-0002-4096-7107

Complete contact information is available at: https://pubs.acs.org/10.1021/acs.langmuir.1c01896

Notes

The authors declare no competing financial interest.

ACKNOWLEDGMENTS

The authors thank H.N.W. Lekkerkerker for useful discussions and suggestions. Dr. C. de Roodt is acknowledged for useful warnings. M.V. acknowledges the Netherlands Organization for Scientific Research (NWO) for a Veni grant (no. 722.017.005).

REFERENCES

(1) Onsager, L. The effects of shape on the interaction of colloidal particles. *Ann. N. Y. Acad. Sci.* **1949**, *51*, 627−659.

(2) Frenkel, D.; Mulder, B. M.; McTague, J. P. Phase diagram of a system of hard ellipsoids. *Phys. Rev. Lett.* **1984**, *52*, 287−290.

(3) Leberman, R. The Isolation of Plant Viruses by Means of "Simple" Coacervates. *Virology* **1966**, *30*, 341−347.

(4) Adams, M.; Fraden, S. Phase Behavior of Mixtures of Rods (Tobacco Mosaic Virus) and Spheres (Polyethylene Oxide, Bovine Serum Albumin). *Biophys. J.* **1998**, *74*, 669−677.

(5) Dogic, Z.; Fraden, S. Development of model colloidal liquid crystals and the kinetics of the isotropic - smectic transition. *Philos. Trans. R. Soc., A* **2001**, *359*, 997−1015.

(6) Dogic, Z.; Purdy, K. R.; Grelet, E.; Adams, M.; Fraden, S. Isotropic-nematic phase transition in suspensions of filamentous virus and the neutral polymer Dextran. *Phys. Rev. E* **2004**, *69*, No. 051702.

(7) Edgar, C. D.; Gray, D. G. Influence of Dextran on the Phase Behavior of Suspensions of Cellulose Nanocrystals. *Macromolecules* **2002**, *35*, 7400−7406.

(8) Oguzlu, H.; Danumah, C.; Boluk, Y. Colloidal behavior of aqueous cellulose nanocrystal suspensions. *Curr. Opin. Colloid Interface Sci.* **2017**, *29*, 46−56.

(9) Buitenhuis, J.; Donselaar, L. N.; Buining, P. A.; Stroobants, A.; Lekkerkerker, H. N. W. Phase Separation of Mixtures of Colloidal Boehmite Rods and Flexible Polymer. *J. Colloid Interface Sci.* **1995**, *175*, 46−56.

(10) Lekkerkerker, H. N. W.; Stroobants, A. Phase behaviour of rod-like colloid+flexible polymer mixtures. *Il Nuovo Cimento D* **1994**, *16*, 949−962.

(11) Bolhuis, P. G.; Stroobants, A.; Frenkel, D.; Lekkerkerker, H. N. W. Numerical study of the phase behavior of rodlike colloids with attractive interactions. *J. Chem. Phys.* **1997**, *107*, 1551−1564.

(12) Savenko, S. V.; Dijkstra, M. Phase behavior of a suspension of colloidal hard rods and nonadsorbing polymer. *J. Chem. Phys.* **2006**, *124*, No. 234902.

(13) Tuinier, R.; Taniguchi, T.; Wensink, H. H. Phase behavior of a suspension of hard spherocylinders plus ideal polymer chains. *Eur. Phys. J. E: Soft Matter Biol. Phys.* **2007**, *23*, 355−365.

(14) Lekkerkerker, H. N. W.; Poon, W. C. K.; Pusey, P. N.; Stroobants, A.; Warren, P. B. Phase Behaviour of Colloid + Polymer Mixtures. *Europhys. Lett.* **1992**, *20*, 559−564.

(15) Lekkerkerker, H. N. W.; Tuinier, R. *Colloids and the Depletion Interaction*; Springer: Heidelberg, 2011.

(16) Buining, P. A.; Lekkerkerker, H. N. W. Isotropic-nematic phase separation of a dispersion of organophilic boehmite rods. *J. Phys. Chem. A* **1993**, *97*, 11510−11516.
(17) Dogic, Z.; Fraden, S. Smectic Phase in a Colloidal Suspension of Semiflexible Virus Particles. *Phys. Rev. Lett.* **1997**, *78*, 2417−2420.
(18) Barry, E.; Dogic, Z. Entropy driven self-assembly of nonamphiphilic colloidal membranes. *Proc. Natl. Acad. Sci. USA* **2010**, *107*, 10348−10353.
(19) Gibaud, T.; Barry, E.; Zakhary, M. J.; Henglin, M.; Ward, A.; Yang, Y.; Berciu, C.; Oldenbourg, R.; Hagan, M. F.; Nicastro, D.; Meyer, R. B.; Dogic, Z. Reconfigurable self-assembly through chiral control of interfacial tension. *Nature* **2012**, *481*, 348−351.
(20) Kuijk, A.; Byelov, D. V.; Petukhov, A. V.; van Blaaderen, A.; Imhof, A. Phase behavior of colloidal silica rods. *Faraday Discuss.* **2012**, *159*, 181.
(21) Grelet, E. Hard-rod behavior in dense mesophases of semiflexible and rigid charged viruses. *Phys. Rev. X* **2014**, *4*, No. 021053.
(22) Gibaud, T.; Kaplan, C. N.; Sharma, P.; Zakhary, M. J.; Ward, A.; Oldenbourg, R.; Meyer, R. B.; Kamien, R. D.; Powers, T. R.; Dogic, Z. Achiral symmetry breaking and positive Gaussian modulus lead to scalloped colloidal membranes. *Proc. Natl. Acad. Sci. USA* **2017**, *114*, E3376−E3384.
(23) Peters, V. F. D.; Vis, M.; Wensink, H. H.; Tuinier, R. Algebraic equations of state for the liquid crystalline phase behavior of hard rods. *Phys. Rev. E* **2020**, *101*, No. 062707.
(24) McGrother, S. C.; Williamson, D. C.; Jackson, G. A re-examination of the phase diagram of hard spherocylinders. *J. Chem. Phys.* **1996**, *104*, 6755−6771.
(25) Bolhuis, P. G.; Frenkel, D. Tracing the phase boundaries of hard spherocylinders. *J. Chem. Phys.* **1997**, *106*, 666−687.
(26) Wensink, H. H. Columnar versus smectic order in systems of charged colloidal rods. *J. Chem. Phys.* **2007**, *126*, No. 194901.
(27) Grelet, E. Hexagonal order in crystalline and columnar phases of hard rods. *Phys. Rev. Lett.* **2008**, *100*, No. 168301.
(28) Grelet, E.; Rana, R. From soft to hard rod behavior in liquid crystalline suspensions of sterically stabilized colloidal filamentous particles. *Soft Matter* **2016**, *12*, 4621−4627.
(29) de Braaf, B.; Oshima Menegon, M.; Paquay, S.; van der Schoot, P. Self-organisation of semi-flexible rod-like particles. *J. Chem. Phys.* **2017**, *147*, No. 244901.
(30) Peters, V. F. D.; Vis, M.; González García, Á.; Wensink, H. H.; Tuinier, R. Defying the Gibbs Phase Rule: Evidence for an Entropy-Driven Quintuple Point in Colloid-Polymer Mixtures. *Phys. Rev. Lett.* **2020**, *125*, No. 127803.
(31) González García, Á.; Tuinier, R.; Maring, J. V.; Opdam, J.; Wensink, H. H.; Lekkerkerker, H. N. W. Depletion-driven four-phase coexistences in discotic systems. *Mol. Phys.* **2018**, *116*, 2757−2772.
(32) Dijkstra, M.; van Roij, R.; Evans, R. Phase diagram of highly asymmetric binary hard-sphere mixtures. *Phys. Rev. E* **1999**, *59*, 5744−5771.
(33) Aarts, D. G. A. L.; Tuinier, R.; Lekkerkerker, H. N. W. Phase behaviour of mixtures of colloidal spheres and excluded-volume polymer chains. *J. Phys.: Condens. Matter* **2002**, *14*, 7551−7561.
(34) Fleer, G. J.; Tuinier, R. Analytical phase diagrams for colloids and non-adsorbing polymer. *Adv. Colloid Interface Sci.* **2008**, *143*, 1−47.
(35) González García, Á.; Opdam, J.; Tuinier, R.; Vis, M. Isostructural solid-solid coexistence of colloid-polymer mixtures. *Chem. Phys. Lett.* **2018**, *709*, 16−20.
(36) González García, Á.; Tuinier, R.; de With, G.; Cuetos, A. Directional-dependent pockets drive columnar-columnar coexistence. *Soft Matter* **2020**, *16*, 6720−6724.
(37) van der Kooij, F. M.; Vogel, M.; Lekkerkerker, H. N. W. Phase behavior of a mixture of platelike colloids and nonadsorbing polymer. *Phys. Rev. E* **2000**, *62*, 5397−5402.
(38) Mederos, L.; Velasco, E.; Martínez-Ratón, Y. Hard-body models of bulk liquid crystals. *J. Phys.: Condens. Matter* **2014**, *26*, No. 463101.
(39) Fasolo, M.; Sollich, P. Effects of polymer polydispersity on the phase behaviour of colloid-polymer mixtures. *J. Phys.: Condens. Matter* **2004**, *797*, 797−812.
(40) Paricaud, P.; Varga, S.; Cummings, P. T.; Jackson, G. Effect of polymer chain-length polydispersity on the phase behavior of model athermal mixtures of colloids and flexible self-excluding polymers. *Chem. Phys. Lett.* **2004**, *398*, 489−494.

https://doi.org/10.1021/acs.langmuir.1c01896
Langmuir 2021, 37, 11582−11591